Inverting Earth Parameters via Forward Modelling to Obtain Apparent Resistivity Pseudosections

GOPH 549

Kristopher Innanen

Brandon Karchewski

Rachel Lauer

Safian Omar Qureshi

ID 10086638

Contents

Abstract

Electrical Resistivity Tomography (ERT) survey was employed on a site near Castle Mountain Resort located in Pincher Creek, Alberta Canada. Preliminary inspection of the site suggests area of low relief plains in valley formation, covered with glacial till composed of a shallow weathering or vegetal top soil layer, likely containing clay that has a high surface area to volume ratio due to its platey geometry and can be suited to holding charge. As such, the specific site is a good candidate to employ an ERT survey; an effective non-destructive imaging tool where direct current is supplied to the subsurface and the potential difference is measured in order to gain an understanding of the intrinsic property resistivity of the medium. This investigation focused on creating an ERT forward modelling algorithm that is used iteratively to perform inversion of user supplied earth parameters to create a defensible model of the subsurface against provided results. Those parameters were found to be resistivities ρ_1 , ρ_2 being 332 Ωm, 865 Ωm of top, bottom layers respectively and an interface depth of 23m. Seismic data was also supplied of the same region and jointly correlating it with the resistivity data lead to concluding lower velocity (952m/s) top layer consisted of unconsolidated dry clays/gravel/sands/soil until a similar depth of 26 meters. Further down, compaction and cementation gave rise to higher velocity (2564m/s) of deeper bedrock layer, most likely consisting of porous saturated sandstones or coal.

Background and Theory

Elementary physics defines a field extending outward from a point source charged particle perpendicular to its surface as the electric field. It determines the electric force exerted by the particle on other charged particles and its strength decreases with distance according to an inverse-square law. The electrical potential is then defined as the amount of work required to move a positive charge from a point outside the influence of the field to some point under the influence of the field (Millikan, 1913). In practice, one Volt (V) is the potential difference between the two points where 1 Joule (J) of work is done by 1 Coulomb (C) of electric charge to go from one point to the other. Electric current is measured in ampere (A) which refers to a flow rate of 1 Coulomb per second. These definitions finally give meaning to Ohm's Law

$$V = IR \qquad (1)$$

where current through two points in any medium is proportional to the voltage across those points; the proportionality constant is known as *R* in Ohm (Ω), resistance for 1 A of electrical current from a potential difference of 1 V (Eaton, 2014).

This resistance makes it possible to increase understanding of the type of medium in which the current flows. The resistance depends on intrinsic properties of the medium which are of interest and extrinsic factors (such as size and shape) which are not. To eliminate factors of disinterest, the medium is assumed to be an isotropic homogenous material. Consider a current *I* flowing through an isotropic homogenous cylinder of length *L* with a cross sectional area of *A*

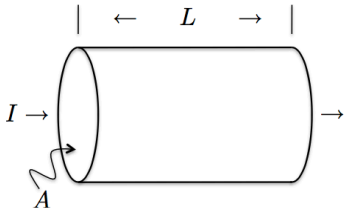

FIG. 1: current flowing through a homogenous isotropic cylinder to show relation with R (Innanen, GOPH 355)

where the resistance can be intuitively (and is empirically) defined as proportional to the length over the cross sectional area (Innanen, 2013). The proportionality is taken care of by constant ρ known as resistivity in units Ωm. This resistivity is of great importance as it defines the intrinsic rock property of the materials in the subsurface. Of all geophysical parameters, resistivity shows the greatest range in values, from 10^{-8} Ωm to 10^{16} Ωm. As such, resistivity ranges of different earth materials often overlap, creating a need to employ resistivity methods alongside another geophysical technique. Large contributing factors to resistivity involve porosity, permeability and type/level of saturation. Porosity is the amount of pore space in the medium and can greatly influence the passage of ions when electrical current flows. Permeability refers to the connectivity of the pores and saturation refers to the type and level of fluid content between pores, where one type of fluid may be more conductive than others, both of which affect resistivity. It is worth to note that air has a theoretical infinite resistivity and will produce large resistive anomalies that are useful in detection of subsurface voids (Cardimona, 2016).

We can now begin passing a current through the subsurface by placing an electrode on top of the surface. Two assumptions include supplying a direct current to an infinite half space below. Additional boundary conditions are required when there is contact between two regions of different conductivity, since air counts as a region (Telford, 1990). Boundary conditions are

$$n\,x\,(E_1 - E_2) = 0 \qquad (2)$$

$$n\,.\,(\sigma E_1 - \sigma E_2) = 0 \qquad (3)$$

where equation (2) refers to electric field tangential to interface must be continuous and equation (3) refers to the current density normal to the interface must also be continuous. Potential *V* at a distance *r* from the current source I is a solution to Poisson's equation, given by

$$V = \frac{I\rho}{2\pi\, r} \tag{4}$$

showing current flowing from a single electrode through a hemispherical infinite surface below (Telford, 1990). Although appropriate in building foundation for mathematical purposes, this equation must be modified as a single electrode stuck in the surface does not complete a circuit. As such, another electrode is needed to complete the circuit and further, we are not interested in potential rather potential difference, ΔV, which would lead to an additional electrode pair being needed to measure it. These electrode pairs can be configured in different collinear configurations, the effect of which we will see later. Because currents at the two electrodes are equal and opposite in direction, we can simply add another term like (4) for each electrode pair 1 and 2, then taking the difference to give us *ΔV* as shown below (Innanen, 2013).

$$V_1 = \frac{I^+\rho}{2\pi\, r_1} - \frac{I^-\rho}{2\pi\, r_2} = \frac{I\rho}{2\pi}\left(\frac{1}{r_1} - \frac{1}{r_2}\right) \tag{5}$$

$$V_2 = \frac{I^+\rho}{2\pi\, r_3} - \frac{I^-\rho}{2\pi\, r_4} = \frac{I\rho}{2\pi}\left(\frac{1}{r_3} - \frac{1}{r_4}\right) \tag{6}$$

$$\Delta V = \frac{I\rho}{2\pi}\left\{\left(\frac{1}{r_1} - \frac{1}{r_2}\right) - \left(\frac{1}{r_3} - \frac{1}{r_4}\right)\right\} \tag{7}$$

Recall the assumption of the half space below the electrodes as an isotropic and homogeneous medium in which the current travels. In reality, the earth does not behave in such a manner. A measured voltage difference yields a resistivity value that is an average over the path length the current follows, the path most likely of heterogenous composition (Innanen, 2013). As such, when rearranging for *ρ*, instead use

$$\rho_a = \frac{2\pi\Delta V}{I}\frac{1}{\left(\frac{1}{r_1} - \frac{1}{r_2}\right) - \left(\frac{1}{r_3} - \frac{1}{r_4}\right)} = \frac{\Delta V}{I}K \tag{8}$$

where ρ_a is referred to as apparent resistivity and *K* is the geometric factor.

A closer look into the geometric factor is worth exploring as it is directly proportional to ρ_a. In order to do so, we must refresh our understanding on what r_1, r_2 r_3 ,r_4 mean and that can be done through a few figures

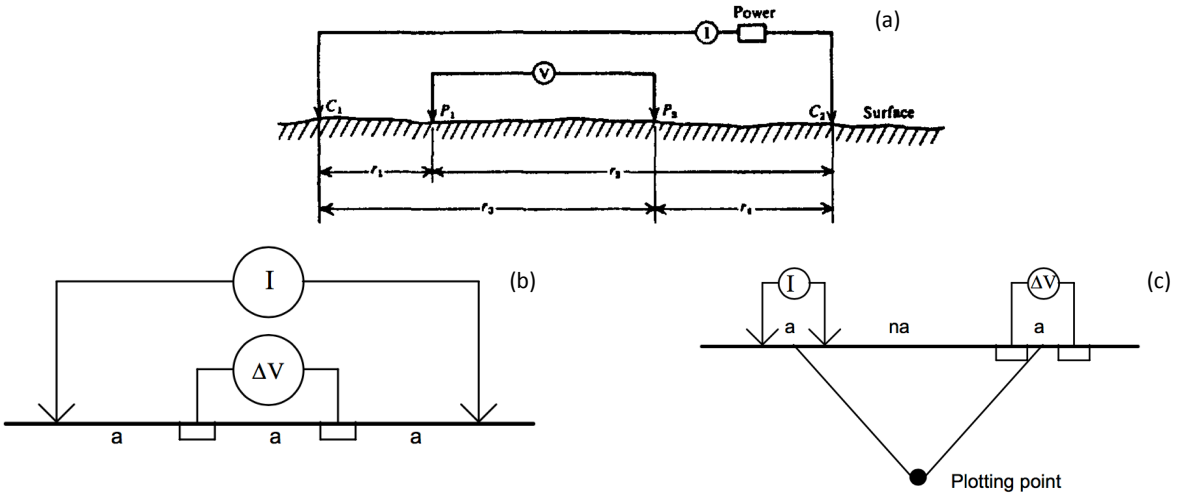

FIG. 2: (a) current and potential electrodes on top of surface, showing r spacings (Telford, 1990). (b) and (c) depict different arrangements of electrodes (wenner and dipole dipole arrays) and how ρ_a would be plotted (Cardimona, 2016).

where C_1, C_2, P_1, P_2 are the current and potential electrode pairs mentioned earlier to measure potential difference. It is apparent now (pun unintentional) that the effects of different configurations of electrodes lead to different geometric factors. These geometric factors can be obtained by some simplification via algebra, recognizing *r* values are n integer multiples of spacing between electrodes. In practice, a line of electrodes are placed and collections of four electrode arrays are activated and scanned automatically in different formats to give apparent resistivity values at plotted points. Pseudosections are generated in such a manner and the algorithm for traversing along the survey line will be explored later.

Consider a two layer system, one layer buried at a finite depth and the lower layer an infinite half space once again. Assumptions are similar: direct current used, boundaries extending infinitely horizontally, homogenous and isotropic medium and boundary conditions from equations (2) and (3) are still relevant. An additional assumption is used where ρ_2 of half space layer is greater than ρ_1 of above finite layer. We can now begin our exploration with a figure that demonstrates the concept of infinite set of images being produced above and below the current electrode due to three mediums being at play. These images have an effect on the potential at point P and must be added together. Equations for the first four images are given further down and a general formula can be constructed intuitively by inspection when the first few are derived empirically.

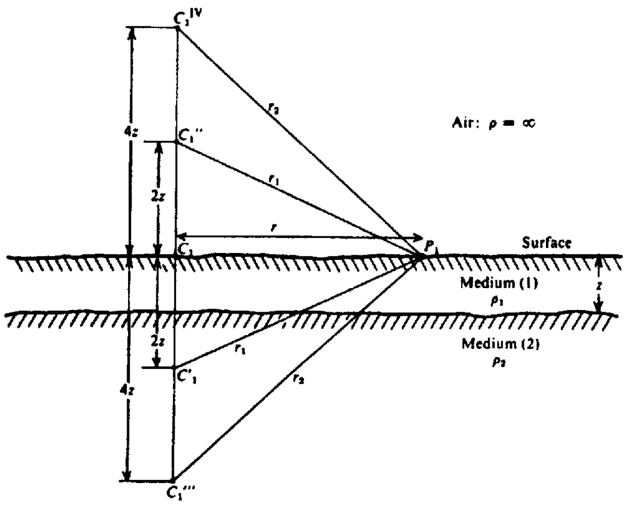

FIG. 3: due to three mediums of differing conductivity, an infinite set of images result (of which 4 are shown) that affect the potential and ultimately the resistivity at a certain point (Telford, 1990).

$$V' + V'' + V''' + V'''' = \frac{I\rho_1}{2\pi}\left(\frac{1}{r}\right) + \frac{I\rho_1}{2\pi}\left(\frac{2k}{r_1}\right) + \frac{I\rho_1}{2\pi}\left(\frac{2k^2}{r_2}\right) \qquad (9)$$

Taking the coefficient out and using summation notation, the resultant total potential at a certain point P can then be expressed as an infinite series of form (Telford, 1990)

$$V = \frac{I\rho_1}{2\pi}\left[1 + 2\sum_{m=1}^{\infty}\frac{k^m}{(1+(2mz/r)^2)^{1/2}}\right] \qquad (10)$$

where k is the reflection coefficient $\rho_2 - \rho_1/\rho_2 + \rho_1$. Recognizing that $|k| < 1$ and the denominator increases indefinitely, the series is deemed to be convergent, which is a point to be taken advantage of in the Matlab implementation. This concludes the study of surface potential due to horizontal beds. Armed with the knowledge of the fundamentals on the background and theory, work can begin constructing an algorithm that repetitively uses equations (8) and (10) depending on which four electrodes are 'active' and in doing so will generate a whole set of values for apparent resistivities at different horizontal and vertical locations used to eventually create pseudosections.

Algorithm Structure and Implementation

A two layer subsurface model must be constructed; top layer buried at a finite depth *z* with lower layer being an infinite half space and the resistivity of it being greater, both mediums isotropic and homogenous. The Matlab implementation begins with a function that calculates ρ_a at a singular point corresponding to each adjacent pair of 'active' potential electrodes. The initial inputs that are passed to the function are position of current and potential electrodes, depth of first interface and resistivities ρ_1, ρ_2. Current *I* is not needed since resistivity will be constant for any current *I* in a homogenous and isotropic medium (Telford, 1990). As such, it is recognized we must work with equations (8) and (10), modifying the latter slightly to find ΔV.

Let's take a look back at equation (8); ρ_a is potential difference ΔV multiplied by the geometric factor *K*, current *I* can be ignored. With inputs being the current and potential locations being passed to the Matlab function, obtaining the geometric factor is fairly simple. By finding the absolute values of the positional differences between the different electrodes, we can simply plug them in as distances r_1, r_2 r_3 ,r_4 into the formula for K and it can be calculated. Obtaining ΔV is not as trivial and the equation for deriving it is as follows (Telford, 1990)

$$\Delta V = V_1 - V_2 = \frac{I\rho_1}{2\pi}\left[\left(\frac{1}{r_1}-\frac{1}{r_2}\right)-\left(\frac{1}{r_3}-\frac{1}{r_4}\right) \quad +2\sum_{m=1}^{\infty} k^m\left\{\frac{1}{(r_1^2+4m^2z^2)^{1/2}} \quad -\frac{1}{(r_2^2+4m^2z^2)^{1/2}} \quad -\frac{1}{(r_3^2+4m^2z^2)^{1/2}} \quad +\frac{1}{(r_4^2+4m^2z^2)^{1/2}}\right\}\right] \quad (11)$$

which is seemingly intimidating though working through it slowly proves otherwise. Current *I* can be ignored, distances r_1, r_2 r_3 ,r_4 are found above, ρ_1 is an input, *z* is an input and *k* is the reflection coefficient. The difficulty lies in the summation but recall from equation (10) that it does in fact converge at some value *m* and as such we only calculate the summation up to that *m.* To find that *m*, an arbitrary small threshold is created as a constant to test how the current *del_sum* varies with the previous given summation of prior terms. A flowchart which was employed in the Matlab implementation is provided to help illustrate the point further.

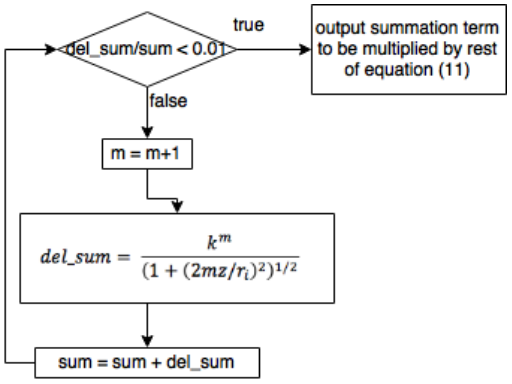

FIG. 4: an important piece of the algorithm in tackling the summation, taking advantage of the fact it converges.

Once that amount of m terms is found and summed, we can add and multiply it to the rest of the equation for ΔV. Once ΔV is found, equation (8) is used to multiply it with K to find ρ_a at that particular point and so the function is complete.

With a function created that will calculate apparent resistivities given initial electrode positions inputs, it is desirable to use that function multiple times for different current and potential electrode positions on the surface. Focusing on the dipole-dipole configuration of electrodes, recall figure 2(c) where the plotting point is created. Before even traversing along the electrode line, it is important to derive where that point will be exactly with regards to x, z position. That position is defined as the intersection point of 45 degree lines centred on the dipoles extending downward (Hallof, 1957). Understanding the geometry, the vertical position of ρ_a can be calculated as

$$z_p = -(\frac{an}{2} + \frac{a}{2}) \qquad (12)$$

and horizontal position of ρ_a can be calculated as

$$x_p = (\frac{x_{2p} - x_{2I}}{2}) \qquad (13)$$

where x_{2p} - x_{2I} is the position of the second potential electrode subtracted by the position of the first current electrode, simply being the midpoint of the four electrode configuration. However, in the Matlab implementation, the electrodes are placed on a cartesian x axis and so a minor adjustment needs to be made where we first add the positions of the potential and current electrodes and then subtract the preceding line, then divide by two.

With knowing how to calculate ρ_a and its corresponding x_p and z_p positions, we can now employ an algorithm to traverse through the electrode line. An excellent animation is available courtesy of The University of British Columbia (link) to provide with a brief visualization as to how looping will occur. The nested inner while loop has the main condition of looping for the number of 'resistive layers', which are provided to us (in the animations case 4 and in our case 10). As such, the inner loop will calculate the ρ_a, x_p and z_p positions and then modify the n integer spacing by one which will allow the potential electrodes to move forward and keep the current electrodes in the same location. It then repeats for that new spacing, calculating the ρ_a , x_p and z_p positions once more, appending those values to newly created vector variables.

Once all the resistive layers and corresponding integer spacings are complete, it breaks out of the loop to reset the integer spacing and move the survey location over one, which affects the current electrodes. The outer while loops condition is to move the survey location over one until the 'maximum' of the survey is reached, determined by if the position of the second outer potential electrode has reached the end. And so once the survey location is moved over and the spacing is reset, the inner loop works again for a different current electrode location, calculating ρ_a , x_p and z_p for each resistive layer and increasing the integer spacing to move the potential electrodes over each time. Once the end of the resistive layers is reached and integer spacing is maxed, ρ_a , x_p and z_p collection of vectors are updated and the outer loop is triggered again to reset spacing and shift survey location once more, affecting the current electrode location position. It is important to employ a secondary condition to the inner while loop which checks if the end of the survey has been reached. If so, then that condition takes precedence over the resistive layer condition so as not to calculate resistivities out of the survey (there would be no electrodes there!).

With this looping algorithm, we can now traverse through the whole line, calculating x_p, z_p positions and ρ_a that are later transformed via Matlab's meshgrid function to plot pseudo sections. Apparent resistivity vs depth is also calculated and plotted against given data. At this point in the Matlab implementation we begin an inversion process, returning back to the initial function that was supplied with the input earth parameters. Tweaking ρ_1 , ρ_2 and z to do forward modelling once more to calculate ρ_a helps strengthen the earth model. Repetitively inverting the parameters and continuously employing the forward modelling algorithm helps even more, resulting in a final model that is close to the given results as shown, at which point we can move ahead to begin exploring the results.

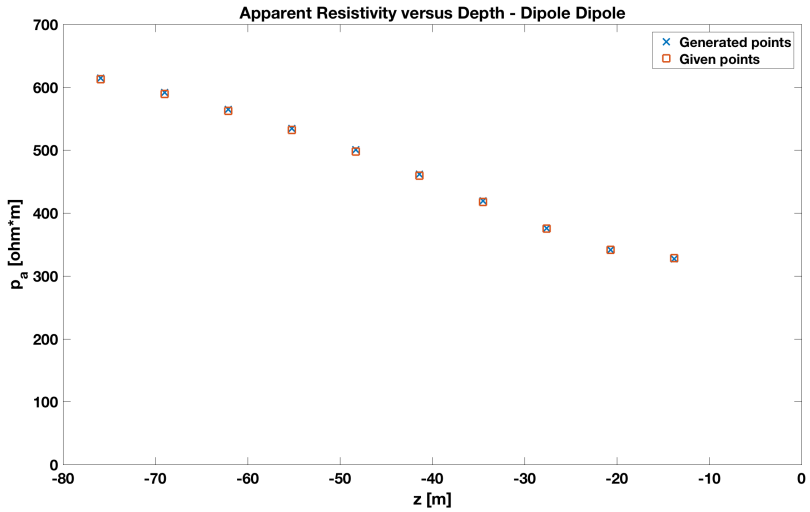

FIG. 5: via inversion of parameters and exhaustive forward modelling, generated values lie close to actual data

Results from Exploring Data

Before trying to interpret the results, it is good practice to have precursory knowledge of the underlying geology of the region that was surveyed. The site was located in the middle of a U-shaped valley with fairly steep sides and a mostly flat bottom in between. Glaciated valleys form by the process of scouring where a glacier travels down a slope carving a valley (MacGregor, 2002). Once the temperature rises past a limit, the ice recedes though the valley remains and the entrainment of the ice leaves deposits known as glacial till. Till is often composed of fairly coarse and heterogenous sediments since it has not had a chance to undergo sorting by the meltwater (Christiansen, 1979).

As such, educated guesses can be made of the top finite layer; it most likely may consist of unconsolidated clay deposits. Clay has a high conductivity due to its geometry and since resistivity is the reciprocal of conductivity, lower resistivity values are to be presumed. This can be expected at smaller electrode spacings and lower depth values, where the current only flows through the upper medium due to the circuit being small. This turns out to be the case in our results where 332 Ωm resistivity was found of the top layer. Like mentioned earlier on, resistivity values often overlap for different materials so another data set can help narrow down the material. Seismic refraction data is provided and velocities can be found to correlate with the resistivity.

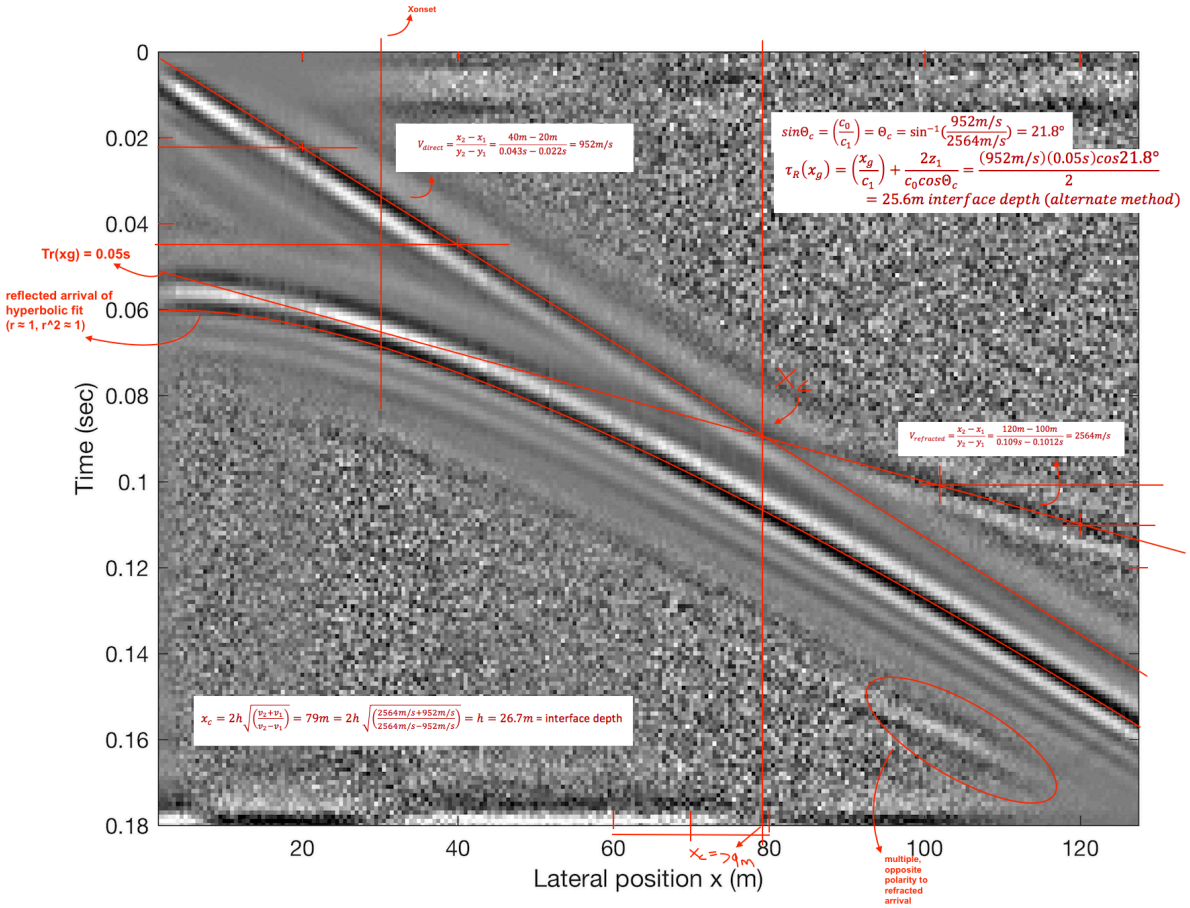

FIG. 6: a refraction data set after being interpreted to find velocity of top and bottom layers along with interface depth.

With the velocity being 952m/s of the top layer, dry sands tend to fall under that category (Mavko, 2014). Gravel and sand tend to have resistivity values between 400 Ωm to an upwards of 10,000 Ωm (Palacky, 1987) . Clays have resistivity values from 10 Ωm to 100 Ωm and velocities from 1000m/s - 2500m/s. A case can be made of the top layer containing an unconsolidated blend of clays, gravel, dry sands and soils in a horizontal fashion. With the setting being a glacial trough, these results are indeed plausible for deposits to mix since till consists of a variety of particle sizes.

At larger electrode spacings, the current can begin travelling through the bottom layer and have a greater depth of penetration due to the circuit now being larger. One can intuitively imagine that more of the lower layer is sampled with greater electrode spacing and so for greater electrode spacings, higher resistivity values are observed given our assumption $\rho_2 > \rho_1$. The depth to the interface was found to be 23m via resistivity methods and ~26m via refraction methods which show a fairly high level of agreement. The bottom half space layer was found to be more resistive with a value of 865 Ωm and a velocity value of 2564m/s. Via tables provided by Mavko and Palacky for velocities and resistivities respectively, jointly correlating the two values narrows down the medium composition; the layer being composed of either porous saturated sandstones or coals.

Even though jointly correlating resistivity and seismic data can help reduce error, it is important to be wary of the limitations. Non uniqueness is common in the field of geophysics and absolute certainty is hard to achieved. Some limitations of the resistivity method include difficult interpretation in the presence of complex geology and the existence of natural currents and potentials in the medium (Cardimona, 2016). Also, we must recall that a measurement obtained at any positional location in the subsurface represents a weighted average of the effects produced over a large volume of material. Nearby geology has a great effect contributing towards that measurement and as such this tends to produce smooth curves which are not ideal for interpretations (Wightman, 2003). Depths as plotted in the pseudo section normally overshoot the true depth of investigation and that should also be taken into consideration. Uneven topography can also play a factor and further corrections such as statics are often required. However, our RMS error of the resistivity methods produced a value of <1.5% in both the Wenner and dipole dipole arrays. As such, in this particular case, the confidence level is modestly high of our qualitative and quantitative results.

Conclusion

ERT surveys are a common tool in geophysical exploration where a line of electrodes is laid of constant spacing along a surface. With the right apparatus, collections of four electrodes can be remotely activated to pass a current through the subsurface. Different configurations have their unique advantages such as further depth penetration or higher shallow resolutions. Due to different configurations, the geometric factor K varies and needs to be taken into consideration given that apparent resistivity is directly proportional to it.

The core of the technique lies in the flow of electrical current and the measuring of potential difference across the electrodes which in turn measures the response of the earth. That response comes in the form of the earth model parameter resistivity. A number of factors affect resistivity such as porosity, permeability and saturation of the subsurface; water playing the greatest role in the shallow subsurface. Measurement of resistivity can often be thought of as the amount of fluid saturation and connectivity of pore space in the real world (Cardimona, 2016). Porous rock of high fractures with empty spaces will be of low conductivity and so high resistivity. Increasing compaction of soils or rocks will counteract porous nature and an increase in resistivity will be observed, as was seen in the results for the bottom layer.

In our case, a homogenous and isotropic medium was assumed for both top and basal half space layers. Final results were concluded to be a top layer extending downward to a depth of ~24.5m, being horizontal in orientation. Taking the geology into account as well as empirical measurements of resistivity (332 Ωm) and velocity (952m/s), a case could be made that the composition consisted of a mixture of dry sands, gravel, clays and soil content. Further down, an increase in resistivity (865 Ωm) and velocity (2564m/s) was observed. Given these two earth parameters, some rocks that fall in that category are porous saturated sandstones or coal and so it can be concluded that the deeper bedrock layer past 25m consisted of such rock types.

As always, there is a level of uncertainty when it comes to geophysical exploration. Sources of error such as topography and noise, along with the inherent limitations of the techniques, can introduce multiple solutions to a problem. This investigation taken as a whole can be thought to illustrate a very important and underlying problem in the field of geophysics; non uniqueness.

References

S. Cardimona, http://www.dot.ca.gov/hq/esc/geotech/geo_support/geophysics_geology/documents/geophysics_2002/061cardimona_resistivity_overview.pdf. 2016: doi:10.18411/d-2016-154

W. M. Telford, L. P. Geldart, L. P. Sheriff, Applied Geophysics, 1990: Cambridge Univ. Press p 530-570

R. A. Millikan, On the Elementary Electrical Charge and the Avogadro Constant. 1913: Physical Review, 2(2), 109-143. doi:10.1103/physrev.2.109

K. A. Innanen, Seismic Amplitudes, Well Logs, and Rock Properties, 2017: Geophysics 355 Course Notes, p 4-6

D. Wang, Physics and Chemistry of the Deep Earth, 2013: Electrical conductivity of minerals and rocks. doi:10.1002/9781118529492

D. W. Eaton, An Introduction to Resistivity, 2017: Geophysics 453 Course Notes, slides 7 - 8

G. Mavko, Conceptual Overview of Rock and Fluid Factors that Impact Seismic Velocity and Impedance, 2014: Stanford Rock Physics Laboratory, slides 2-3.

P. V. Sherma, Environmental and Engineering Geophysics, 1997: Cambridge, Cambridge University Press, 500 p.

P. G. Hallof, On the interpretation of resistivity and induced polarization measurements, 1957: Cambridge, MIT, Ph.D. thesis.

K. R. MacGregor, Modeling and field constraints on glacier dynamics, erosion, and alpine landscape evolution: 2002

E.A Christiansen, The Wisconsinan Deglaciation of Southern Saskatchewan and Adjacent Areas, 1979 Canadian Journal of Earth Sciences 116: 913–38

D.E. Sudden, B.S. John, Glaciers and Landscape, 1976: London Press.

W. E. Wightman, F. Jalinoos, P. Sirles, K. Hanna, Application of Geophysical Methods to Highway Related Problems. 2003: Federal Highway Administration, Central Federal Lands Highway Division, Lakewood, CO, Publication No. FHWA-IF-04-021